

Supplementary Materials

Experimental Demonstrations of Coherence de Broglie Wavelength for Scalable Superresolution with Near-perfect Fringe Visibility

S. Kim and Byoung S. Ham

Section A

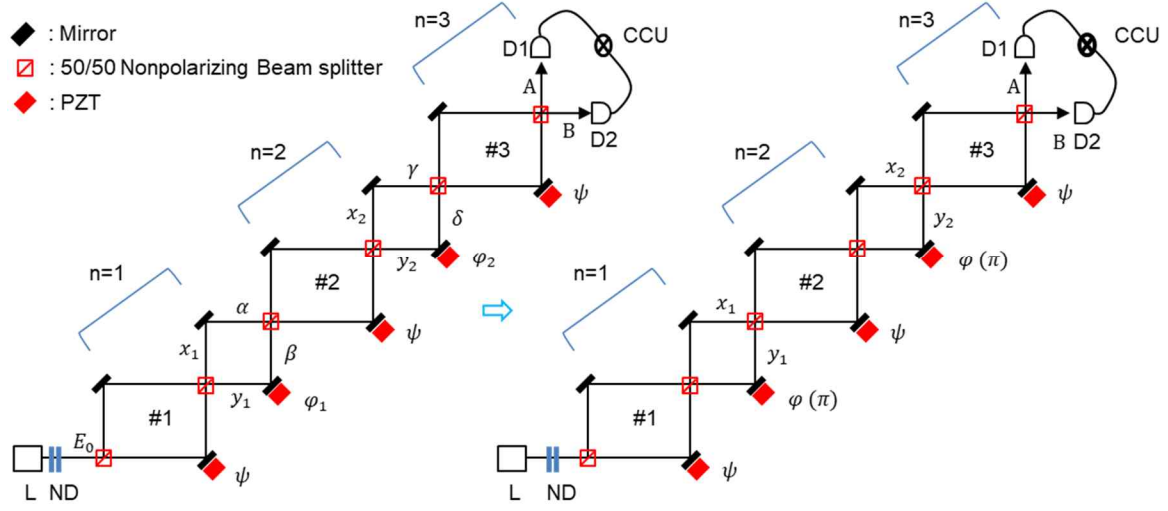


Fig. S1. Schematic of quintuply coupled MZIs for CBWs.

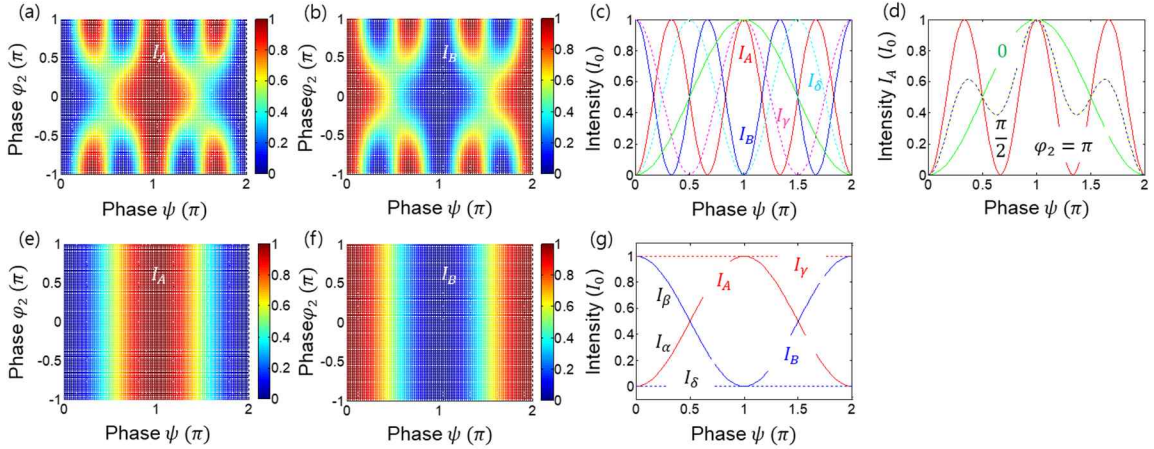


Fig. S2. Numerical simulations for Fig. S1. (a)~(d) $\varphi_1 = \pi$. (e)~(g) $\varphi_1 = 0$. In (c) and (g), $\varphi_2 = \pi$.

Figure S2 shows numerical demonstrations of Fig. S1 for a particular value of φ_1 . This is to understand the mechanism of CBWs in a multiply coupled MZIs. For $\varphi_1 = \pi$, the first three MZIs satisfy a CBW only if $\varphi_2 = \pm\pi$, resulting in CBWs as shown in Figs. S2(a)~S2(c). However, if $\varphi_2 \neq \pm\pi$, the CBW condition is broken as shown in Figs. S2(a) and S2(b). As shown in Fig. S2(d), the phase basis quantization at $\psi = \pi/3$, the correlation efficiency of CBW drops down as the error of φ_2 increases away from $\varphi_2 = \pi$, resulting in φ_2 -dependent outputs. At $\varphi_2 = 0$, the system turns out to be an identity relation between #2 and #3 MZIs as shown in USCKD. In this case, the outputs of Fig. S1 are the same as those in the first MZI (#1) (see the green curve in Figs. S2(c) and S2(d)).

For $\varphi_1 = 0$, Fig. S1 maximally violates the CBW condition, resulting in the identity relation of USCKD between the input of the first MZI (#1) and the output of the third MZI (#3) as shown in Figs. S2(e)~(g). In other words, I_γ is identical to I_0 as shown in the dotted lines of Fig. S2(g). Thus, the last outputs of I_A and I_B show the same results as in a single MZI, resulting in φ_2 independent as shown in the solid curves in Figs. S2(e) and (f).

Section B

1. SPCM-Oscilloscope analysis

Figure S4 shows visualizations of photon distribution resulting from a post-selection technique via coincidence detection. Figure S4(a) and (b) represent the original detection results by SPCMs for attenuated laser split by a 50/50 nonpolarizing beam splitter. Each measured single photon detection rate is 1,015 and 1,028 cps per ms, where each SPCM cannot resolve photon numbers. Figures S4(c) and (d) show coincidentally detected photon pairs, where the details are shown in Fig. S5. These originally paired photons are only counted for the coincidence detection results, where the higher photon numbers, e.g., three or four bunched photons are neglected from the Poisson distribution discussed in Section B-1. In other words, the doubly bunched photons only selected for the coincidence detection measurement in Fig. 2, satisfying sub-Poisson photon distribution with an error of 1% due to inclusion of three or more bunched photon cases: $(\Delta n)^2 \ll \langle n \rangle$.

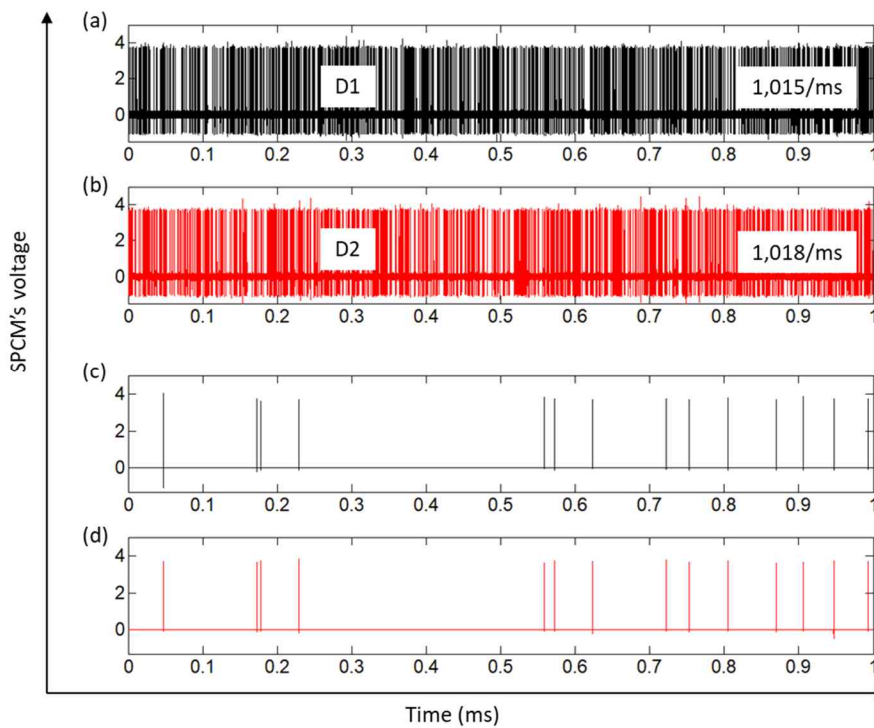


Fig. S4. Nearly sub-Poisson distributed photon streams. (a) and (b) Captured single photon data in the upper path (D1) and lower path (D2) of the first MZI in Fig. 1, respectively. (c) and (d) Measured coincident photon pairs between (a) and (b). Matlab converted oscilloscope data.

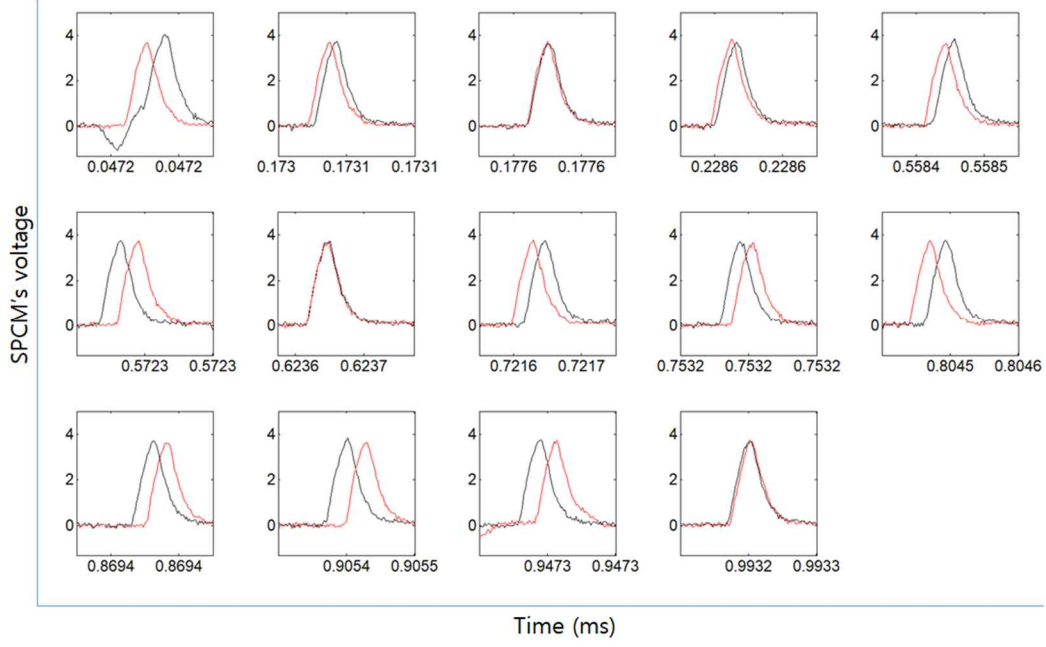


Fig. S5. Details of the coincidently propagating photon pairs in Figs. S3(c) and (d).

2. Poisson statistics

The coherent state $|\alpha\rangle$ and the corresponding probability P_n of finding n photons in quantum mechanics is defined as:

$$|\alpha\rangle = \sum_{n=0}^{\infty} \frac{\alpha^n}{\sqrt{n!}} e^{-\frac{|\alpha|^2}{2}} |n\rangle, \quad (\text{S-1})$$

$$P_n = \frac{\langle n \rangle^n}{n!} e^{-\langle n \rangle}, \quad (\text{S-2})$$

where $|n\rangle$ is a Fock state and $\langle n \rangle$ is the mean photon number. Figure S3 is numerical calculations of equation (S-2) for sub-Poisson photon distribution. Thus, the experimental condition with attenuated laser in Fig. 1 is for quantum particles of sub-Poisson distributed single photons. Moreover, the coincidence detection is for the bunched photon pair, which is far less than 1% of mean photon number in each path of an MZI than the non-coinciding single photons streams measured by D1 and D1 in Table 1.

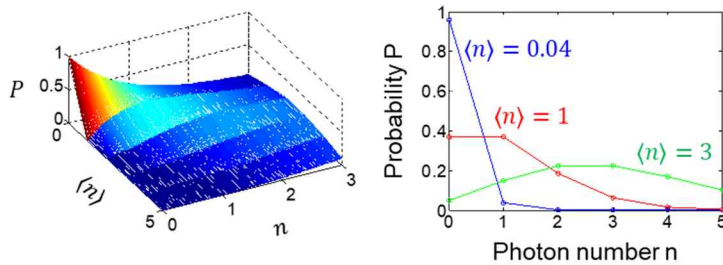


Fig. S3. Numerical simulations for photon statistics of coherent state. For $\langle n \rangle = 0.04$, the probability ratio of $n=2$ to $n=1$ is 2%: $0.00077/0.0384=0.02$. The probability ratio of $n=3$ to $n=2$ for $\langle n \rangle = 0.04$ is 0.01:

$0.00001/0.00077=0.013$. Thus, the single photon stream in each path of MZI has an error of $\sim 2\%$ due to the higher order bunched photons. Compared with the measured data in Table 1 for 0.1 Mcps, the measurement ratio of $n=2$ to $n=1$ is 0.15 %, which is much lower than that for $\langle n \rangle = 0.04$. Thus, the actual mean photon number achieved from the attenuated 532 nm laser is better to use it for quantum particles.

Section C

Figure S6 shows an extreme case of CBW for USCKD [32], where there is an identity relation between the input and output in Fig. 1 when the symmetric MZI configuration is satisfied with $\varphi = 0$ in Fig. 1 between the #1 and #2 MZIs.

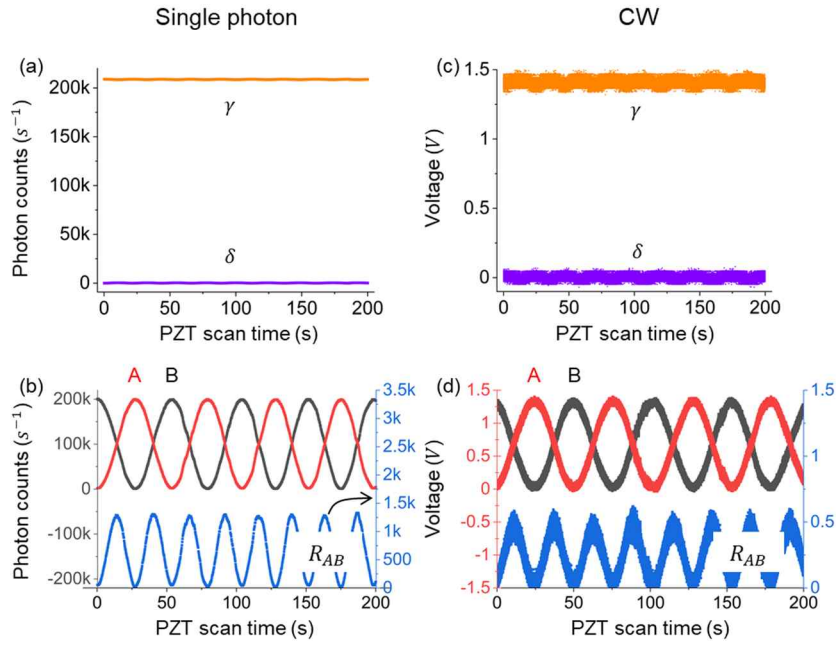


Fig. S6. Experimental demonstration of CBWs for $\varphi = 0$ in Fig. 1. (a) and (b) Single photons. (c) and (d) cw lights.

Figure S7 is for numerical calculations for Fig. S6, where the results coincide.

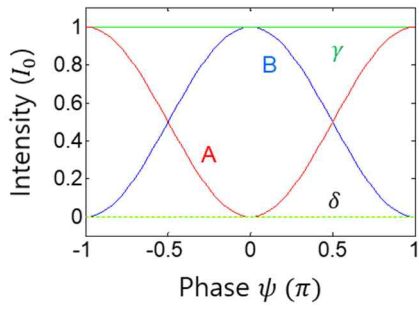


Fig. S7. Numerical calculations of CBWs for $\varphi = 0$ in Fig. 1.